Langmuir

Article

pubs.acs.org/Langmuir

Ordered Self-Assembled Locked Nucleic Acid (LNA) Structures on Gold(111) Surface with Enhanced Single Base Mismatch Recognition Capability

Sourav Mishra, Srabani Ghosh, and Rupa Mukhopadhyay*

Department of Biological Chemistry, Indian Association for the Cultivation of Science, Jadavpur, Kolkata-700032, India

Supporting Information

ABSTRACT: Locked nucleic acid (LNA) is a conformationally restricted nucleic acid analogue, which is potentially a better alternative than DNA for application in the nucleic acid based biosensor technologies, due to its efficient and sequence-specific DNA/RNA detection capability and lack of molecule−surface interaction on solid surfaces, compared to DNA. We report, for the first time, a straightforward way (based on simple immersion method) of generating an ordered self-assembled LNA monolayer, which is bioactive, onto a gold(111) surface. This layer is capable of giving rise to a stronger DNA recognition signal (4−4.5 times) than its DNA counterpart, and importantly, it can differentiate between a fully complementary DNA target and that having a single base mismatch, where the mismatch discrimination ratio is almost two times compared to the ratio relevant in case of DNA-based detection. We have presented high-resolution atomic force microscopy (AFM) topographs of the well-defined one-dimensional LNA molecular ordering (few hundred nanometers long) and of the two-dimensional ordered assembly formed over a large area (7 μm × 7 μm) due to parallel positioning of the one-dimensional ordered arrangements. The effects of different parameters such as LNA concentration and incubation time on LNA self-assembly have been investigated. Further, reflection absorption infrared (RAIR) spectroscopy has been applied to obtain information about the orientation of the surface-immobilized LNA molecules for the first time. It has been found that the LNA molecules undergo an orientational transition from the "lying down" to the "upright" configuration in a time scale of few hours.

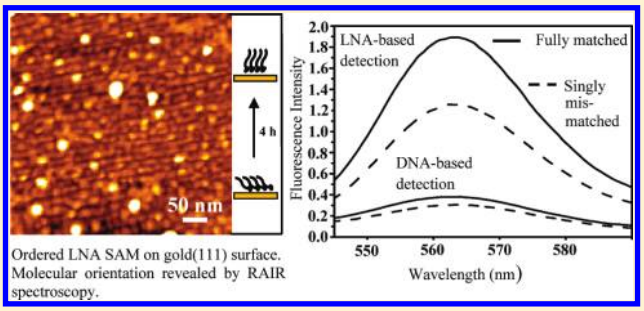

Ordered LNA SAM on gold(111) surface. Molecular orientation revealed by RAIR spectroscopy.

INTRODUCTION

The self-assembled monolayers (SAMs) of biomolecules, especially nucleic acids, onto solid surfaces have drawn much attention during the past decade due to their applicability in many areas of science, especially biosensor development,[1−4] bioelectronics applications,[5,6] and interdisciplinary areas such as nanoscience and nanotechnology.[7−10] Self-assembly provides a fast and straightforward way to produce biomolecular films with tailored properties, particularly those required for development of biosensors. Systematic designing of such films requires molecular level understanding of the structural and functional properties of these films, since it is often found that the nature of the molecular organization can influence the film's capacity of being bioactive.[11]

There have been several studies that report DNA SAM formation on a gold(111) surface using the thiolated ssDNA molecules.[12−15] However, though the DNA films can be routinely generated by immobilizing the thiolated ssDNA molecules onto a gold surface, these films are usually disordered or the ordering can be observed over a very small length scale of 10−50 nm.[16] Poorly ordered DNA layers show reduced bioactivity due to DNA−surface interactions through relatively exposed nucleobases.[12,16,17] Construction of mixed monolayers through the coimmobilization of spacer thiols may also be required for successful DNA-based biosensing.[12] An alternative nucleic acid analogue that least interacts with the substrate surface is necessary to grow bioactive SAMs with efficient DNA recognition capability. Locked nucleic acid (LNA) is a conformationally restricted nucleotide analogue containing a modified ribose moiety in which the 2′-oxygen and 4′-carbon are linked by a methylene bridge, locking the sugar in a RNA mimicking sugar conformation (N-type).[18,19] LNA is capable of sequence-specific binding with complementary DNA/RNA obeying the Watson−Crick base pairing rule with higher affinity and capability compared to DNA, which is reflected in the higher T_m value for LNA−DNA/LNA−RNA duplex compared to that for DNA−DNA/DNA−RNA duplex.[18,19] In addition to that, LNA is stable against nuclease mediated cleavage,[20,21] its higher structural rigidity may prevent interactions with the solid substrate surface,[22] and it can have multiple water bridges that provide it with extra stability compared to DNA or RNA.[23] Also, LNA is a suitable molecule for the analysis of single nucleotide polymorphism (SNP) in solution medium.[24] These properties of LNA make it

Received: October 14, 2011
Revised: February 1, 2012
Published: February 6, 2012

potentially a better alternative than DNA in nucleic acid based detection technologies. Though the applications of DNA SAMs in the microscale as well as nanoscale nucleic acid sensing experiments have been reported,[25−28] more sensitive and robust detection is required that we expect to be achieved using LNA.

Herein, we report the formation of an ordered self-assembled monolayer of ssLNA molecules over a large area (7 μm × 7 μm) on a gold(111) surface, which is stable at ambient conditions and is bioactive. High-resolution atomic force microscopy (AFM), reflection absorption infrared (RAIR) spectroscopy, and fluorescence spectroscopy were employed for structural and functional characterization of the self-assembled structures. To our knowledge, this is the first report on the formation of an ordered LNA SAM, where the LNA molecules can be oriented upright, and where the layer can produce a DNA recognition signal 4−4.5 times stronger than the signals obtained from a DNA-based assay. Moreover, single base mismatch in the target DNA sequences could be discriminated at a ratio almost two times higher than the ratio relevant in the case of DNA-based detection.

MATERIALS AND METHODS

Preparation of LNA Solution. We employed 12-mer ssLNA sequences, having a $-(CH_2)_6SH$ group at the 5′-end to immobilize the

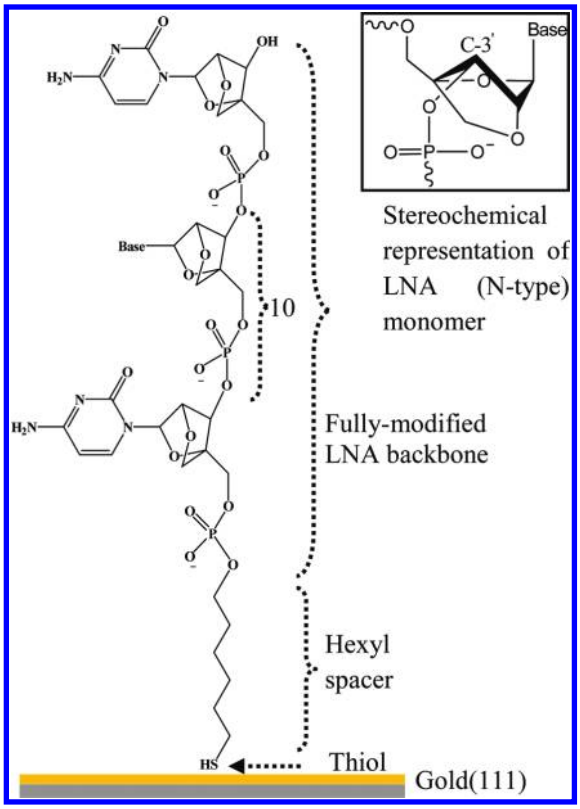

Figure 1. Design of the ssLNA sensor probe.

molecule onto the gold(111) surface (Figure 1). The LNA (Exiqon, Denmark) solutions were prepared in phosphate buffer (20 mM sodium phosphate, 100 mM sodium chloride, pH 7.0). The buffer solution was always prepared using filtered autoclaved Milli-Q water (resistivity: 18.2 MΩ cm). The actual concentration of the prepared LNA solution was determined by UV−visible spectroscopy at room temperature (24 ± 1 °C), considering the absorbance value at 260 nm (ε_{260} (L/(mol × cm)) for LNA-1 to be 112700, for LNA-2 to be 118100, and for LNA-3 to be 111100).

The following fully modified LNA oligonucleotides were employed in this study:

5′- SH-$(CH_2)_6$-CTA TGT **C**AG CAC-3′ (LNA-1)
5′- SH-$(CH_2)_6$-CTA TGT **A**AG CAC-3′ (LNA-2)
5′- SH-$(CH_2)_6$-CGA TCT GCT AAC-3′ (LNA-3)

LNA-1 and LNA-2 were the sensor probes - LNA-1 being the probe for complete match situation and LNA-2 being the probe for single base mismatch situation. LNA 3 was a fully noncomplementary probe used for control experiments.

Preparation of DNA Solution. Thiolated DNA (alpha DNA, Canada) and Cy3 tagged DNA (IDT, Canada) solutions were prepared in phosphate buffer (20 mM sodium phosphate, 100 mM sodium chloride, pH 7.0). The buffer solution was prepared using filtered autoclaved Milli-Q water (resistivity: 18.2 MΩ cm). The actual concentration of the prepared DNA solution was determined by UV−visible spectroscopy at room temperature (24 ± 1 °C), considering the absorbance value at 260 nm (ε_{260} (L/(mol × cm)) for DNA-1 to be 123020, for DNA-2 to be 131350, and for Cy3-DNA to be 124400).

Cy3 is a water-soluble fluorescent dye of the cyanine dye family and is widely used in biomedical applications. Cy3 dye can be excited maximally at ∼550 nm, with peak emission at ∼570 nm.[29,30] In our case, the maximum absorption/excitation wavelength of the Cy3 dye was found to be 530 nm and emission observed at 563 nm.

The following DNA oligonucleotides were employed in this study:

5′- SH-$(CH_2)_6$-CTA TGT **C**AG CAC-3′ (DNA-1)
5′- SH-$(CH_2)_6$-CTA TGT **A**AG CAC-3′ (DNA-2)
5′- Cy3-GTG CTG ACA TAG-3′ (Cy3-DNA)

DNA-1 and DNA-2 were the sensor probes, with DNA-1 being the probe for complete match situation and DNA-2 being the probe for single base mismatch situation. Cy3-DNA was the target probe.

Preparation of Gold(111) Surface. Gold on mica (Phasis, Switzerland) substrate (thickness of gold layer: 200 nm) was flame annealed until a reddish glow appeared. This procedure was repeated 7−8 times and after a short period (1−2 s) of cooling in air the substrate was subjected to further modification steps or imaging. The generation of clean and triangular terraces of high quality gold(111) surface due to flame annealing was checked by AFM imaging at ambient conditions.

Sample Preparation for AFM. Freshly annealed gold on mica substrate was immersed in 150 μL of LNA solution of desired concentration (0.05/0.1/0.25/0.5 μM) and incubated for 4 h for the concentration dependence study. For the incubation time dependence study, freshly annealed gold on mica substrate was immersed in 150 μL of LNA solution of 0.1 μM concentration and incubated for few minutes to few hours (10 min/30 min/1 h/4 h). Sample preparation was always performed at room temperature (24 ± 1 °C). After the incubation step was over, the substrate was first washed with 1 mL (2 × 500 μL) of buffer solution (20 mM sodium phosphate, 100 mM sodium chloride, pH 7.0) followed by 2 mL (4 × 500 μL) of filtered autoclaved Milli-Q water and then dried under gentle nitrogen jet and imaged by AFM at ambient conditions (room temperature 24 ± 1 °C and humidity value of 40−45%).

AFM Data Acquisition and Analysis. All the images were recorded at ambient conditions. AFM experiments were performed using the picoLE AFM equipment of Agilent Corp. with a 10 μm × 10 μm scanner. Imaging was performed in the intermittent contact mode (acoustic alternating current or AAC). The cantilevers (μmasch, Estonia) having the backside coated with Al, frequencies within 150−232 kHz, and force constant values 3.5−12.5 N/m were used for all the imaging experiments. The AFM tips were cleaned in a UV-ozone cleaner (Bioforce, Nanosciences) immediately before imaging. The scan range was made zero during the tip engage step to avoid tip contamination. The amplitude set point was 85−90% of the free oscillation amplitude (7.5−8.0 V). Scan speed was typically 0.5−4.0 lines/s. The AFM images were taken at least from five different areas of each sample to check for reproducibility of the features observed.

dx.doi.org/10.1021/la204026j | Langmuir 2012, 28, 4325−4333

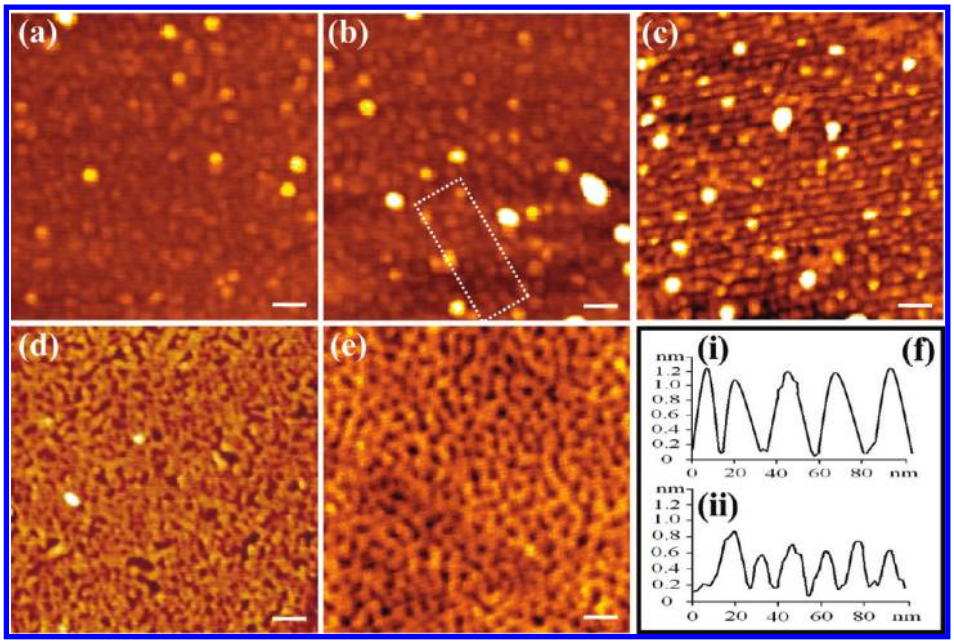

Figure 2. AFM topographs of the LNA-coated gold surface for different LNA concentrations, at room temperature (24 ± 1 °C) and for 4 h incubation time: (a, b) 0.05 μM, (c) 0.1 μM, (d) 0.25 μM, (e) 0.5 μM. Scale bar for (a–e) is 50 nm and *Z*-range for (a) 0–2.2 nm, (b) 0–2.1 nm, (c) 0–2.4 nm, (d) 0–1.9 nm, (e) 0–2.0 nm. (f) Cross-sectional diagrams are for sections taken (i) across the parallel LNA ribbons, (ii) along the long axis of one LNA ribbon. A region showing initiation of the molecule-by-molecule ordering of LNA is highlighted in (b).

All the images presented here are topographic and are raw data except for minimum processing limited to third order flattening. The length of the LNA ribbons was obtained by measuring contour length along a segmented line through the long axis of the ribbon. The width values were measured as full width at half-maximum (fwhm) of the cross-sectional profile drawn along the short axis of the LNA ribbon or along the central region of the LNA molecule, as the case may be. The height values were measured as the difference between highest point of the cross-section diagram and the average baseline representing the substrate surface. All the cross-sectional analyses and processing were made using Picoscan 5.3.3 and SPIP 4.8.1 software. The dimensional analyses were performed on 100 molecules from different images.

Sample Preparation for RAIR Spectroscopy Experiments. All the four samples (for four incubation time periods, i.e., 10 min/30 min/1 h/4 h) were prepared by immersion incubation method as described before (see section 4).

RAIR Spectroscopy Data Acquisition and Analysis. All the RAIR spectroscopic data were recorded on a commercial Nicolet Magna-IR system 750 Series II spectrometer equipped with a liquid nitrogen-cooled MCT detector, at ambient conditions at room temperature (24 ± 1 °C). The external beam was focused on the sample, with a mirror, at an optimal incident angle. The light reflected at the sample was then focused onto a detector. The spectra were recorded within 3200–800 cm^{-1}.

Target Hybridization and Fluorescence Intensity Measurement. Two pieces of gold on mica substrate (from the same stock and of same size) were freshly annealed, and one piece each was immersed into each of 150 μL of 0.1 μM LNA-1 and LNA-2 solutions and kept at ambient conditions for 4 h. After incubation, each of the LNA-modified gold pieces was taken out and washed with 1 mL (2 × 500 μL) of sodium phosphate buffer followed by 2 mL (4 × 500 μL) of filtered autoclaved Milli-Q water in order to remove the nonspecifically adsorbed molecules and dried under gentle nitrogen jet. Then, each of the LNA-modified gold pieces was subjected to hybridization step by incubating into 150 μL of 1 μM Cy3-DNA solution for 1 h at room temperature (24 ± 1 °C). Next, the gold pieces were taken out from the hybridizing solution and washed thoroughly with 1 mL (2 × 500 μL) of sodium phosphate buffer followed by 2 mL (4 × 500 μL) of filtered autoclaved Milli-Q water to remove the nonspecifically bound target molecules and dried under mild nitrogen jet. Then, the fluorophore labeled oligonucleotides (Cy3-DNA) were dehybridized by placing each of the gold pieces into 450 μL of sodium phosphate buffer and heating the buffer solution to 70 °C (we found this temperature to be considerably higher than the melting temperatures of the surface-confined LNA–DNA duplexes, which are ∼50 and ∼29 °C for the fully matched and the singly mismatched duplexes, respectively, in one of our recent ongoing work) for 15 min. After 15 min, the gold piece was taken out from the buffer solution and complete removal of the target DNA strands from the surface was confirmed by fluorescence imaging with Olympus IX61 fluorescence microscope. Then the fluorescence intensity of the dehybridized target DNA solutions was measured by excitation at 530 nm using a Hitachi F-2500 fluorescence spectrometer. Determination of differences in fluorescence intensities of the dehybridized target DNA samples obtained from the LNA–DNA fully matched duplexes and the singly mismatched duplexes was made on the basis of the intensity of the emission maximum. Exactly same protocol was applied for assessing the hybridization efficiency of a DNA-based sensor setup where the DNA-1 and DNA-2 were taken as the sensor molecules.

■ RESULTS

In the present work, the formation of ordered self-assembled LNA structures on gold(111) surface with efficient DNA recognition capability, has been achieved. High-resolution AFM was employed to obtain molecularly resolved information on how the LNA concentration (0.05 μM, 0.1 μM, 0.25 μM, 0.5 μM) and the incubation time (10 min, 30 min, 1 h, 4 h) could affect the characteristics of the LNA film. RAIR spectroscopy was used in order to obtain an idea about how the molecular orientation changed with increase in incubation time period. Fluorescence spectroscopy was applied to assess the degree of hybridization efficiency of the LNA layer and its capability of single base mismatch recognition, compared to a DNA layer. Three 12-mer thiolated ssLNA sequences, named as LNA-1, LNA-2 and LNA-3, were employed as the sensor probes. LNA-1 and LNA-2 were the fully complementary and the single base mismatch sequences, respectively. LNA-3 was the fully noncomplementary sequence and was used as a control. A

dx.doi.org/10.1021/la204026j | *Langmuir* 2012, 28, 4325–4333

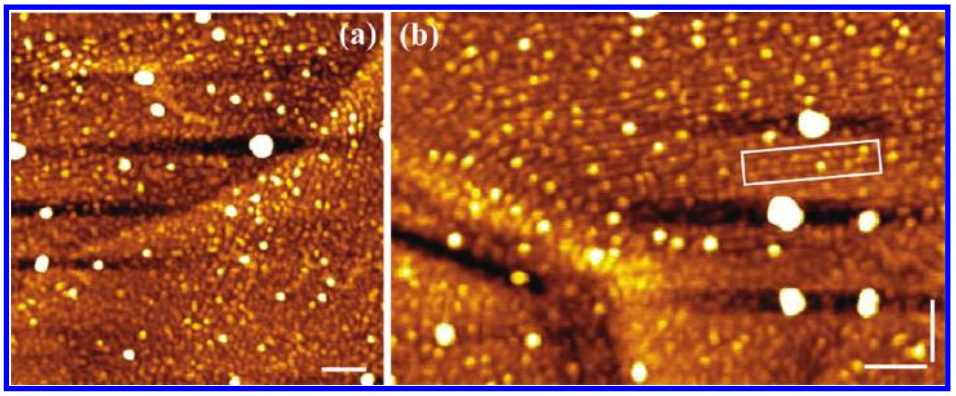

Figure 3. Long range ordering of LNA molecules on gold(111) surface showing change of direction. LNA concentration of 0.1 μM and incubation time of 4 h were applied in both cases (a) and (b). Scale bar for (a) 100 nm, (b) along *X*-axis 100 nm and along *Y*-axis 100 nm. *Z*-range for (a) 0−2.4 nm, (b) 0−2.5 nm.

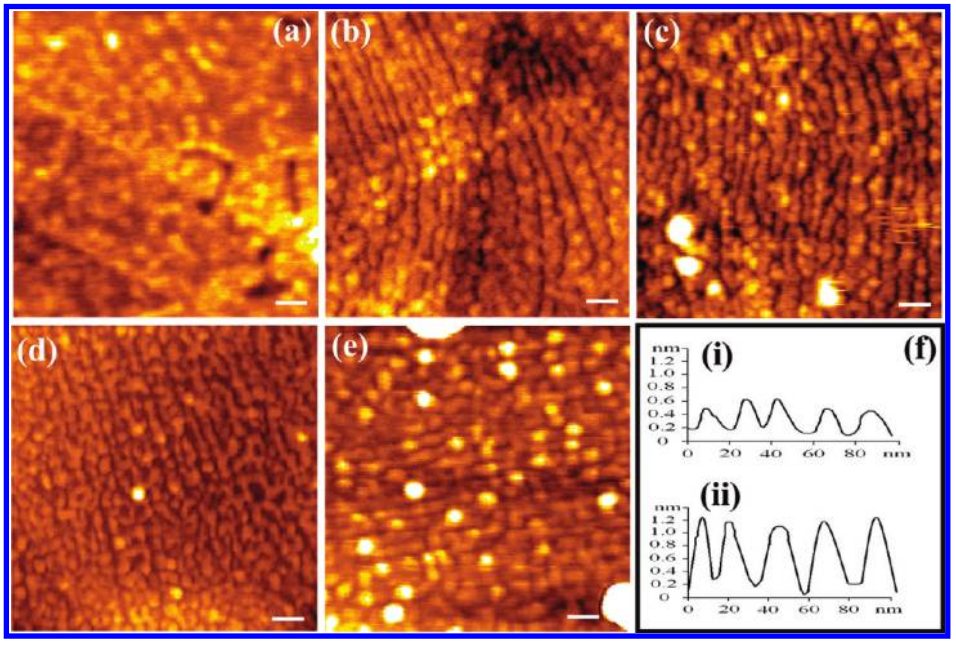

Figure 4. AFM topographs of LNA-modified gold surface for different incubation time periods: (a) 10 min, (b, c) 30 min, (d) 1 h, (e) 4 h. LNA concentration was 0.1 μM in each case. Scale bar for (a−e) is 50 nm. *Z*-range for (a) 0−1.9 nm, (b) 0−2.0 nm, (c) 0−2.1 nm, (d) 0−2.3 nm, (e) 0−2.5 nm. (f) Cross-sectional diagrams are for (i) across the parallel ribbons at 30 min, when the ribbon formation starts, (ii) across the parallel ribbons at 4 h, the highest applied time of incubation.

12-mer 5′-Cy3 tagged ssDNA (Cy3-DNA) sequence, which was fully complementary to LNA-1, was employed as the target strand. Two DNA sequences DNA-1 and DNA-2 having the same base sequence as LNA-1 and LNA-2, respectively, were applied as the DNA counterparts of the LNA probes. In all the sensor molecules, a hexyl spacer [$-(CH_2)_6-$] was introduced at the 5′-end, which helps to keep the nucleic acid part away from the gold surface so that nonspecific adsorption via nucleobases can be avoided to a considerable extent. Since cleanliness of the gold substrate is an absolute requirement for effective anchoring of the LNA molecules via thiol (−SH) ends, the gold pieces were always freshly annealed prior to LNA modification.[31] In all cases, the samples were prepared by immersion incubation method due to it is effectiveness over droplet contact and droplet deposition methods that has been shown previously.[32] All the AFM experiments were performed at ambient conditions, and in the intermittent contact mode using acoustic AC signal.

Effect of LNA Concentration. In order to investigate the concentration dependence of LNA self-assembly on gold substrate, freshly annealed gold substrates were immersed into LNA solutions of various concentrations (0.05 μM, 0.1 μM, 0.25 μM, 0.5 μM) and incubated at room temperature (24 ± 1 °C) for 4 h uninterrupted. For the lowest employed LNA concentration of 0.05 μM, generally scattered LNA molecules were observed all over the surface (Figure 2a). Rarely, the initiation of the molecule-by-molecule ordering could be observed (Figure 2b). This linear arrangement of the LNA molecules that we termed as "LNA ribbon" could be detected in great numbers for the concentration 0.1 μM (Figure 2c). The LNA ribbons were found to be few hundred (100−300) nm in length and they usually formed well-ordered parallel arrangements producing two-dimensional ordered monolayer over a large area (7 μm × 7 μm) of gold surface. The ordered monolayer, where individual molecular identities could be resolved, was not observed when the concentration was raised to 0.25 and 0.5 μM. A highly dense molecular layer, most likely

dx.doi.org/10.1021/la204026j | *Langmuir* 2012, 28, 4325−4333

formed as a result of an increased molecular coverage and multilayer formation on gold substrate, was observed at these concentrations (Figure 2d and e). Accordingly, the optimal LNA concentration for monolayer formation is between 0.1 and 0.25 μM. The average height value of the LNA ribbons was found to be about 1.3 nm (see the cross section profiles in Figure 2f). Though changes in the direction of the ordered patterns could be observed, no clearly distinguishable domains, which were separated by clear domain boundaries, could be identified (Figure 3).

Effect of Incubation Time. The effect of incubation time was monitored by incubating freshly flame annealed gold substrates into LNA solution of 0.1 μM concentration at room temperature (24 ± 1 °C) for the time periods of 10 min, 30 min, 1 and 4 h. For the incubation period of 10 min, generally isolated LNA molecules, scattered all over the surface, were observed, along with initiation of very small range ordering at a few places (Figure 4a). After incubation of 30 min, a greater number of LNA molecules were found to be adsorbed on the gold surface. Long range molecular ordering, leading to formation of long LNA ribbons (100−300 nm in length), was observed at this stage of incubation. Furthermore, the ribbons were found to be positioned almost parallel to each other resulting in formation of a two-dimensional ordered arrangement (Figure 4b and c). The minimum incubation time in order to achieve an ordered LNA SAM over a large area of gold surface was therefore found to be 30 min. The two-dimensional ordered patterns were observed for the incubation time periods of 1 and 4 h (Figure 4d and e). At higher magnification, it could sometimes be resolved that each ribbon consisted of the LNA molecules, positioned one after another, along the long axis of the ribbon (one such situation is shown in the highlighted region in Figure 3b). The average AFM height value of the ribbons changed from 0.72 to 1.3 nm as the incubation time was increased from 30 min to 4 h (Figure 4f). The increase in the height value might be associated to a change in the orientation of the LNA molecules from the "lying down" to the "upright" one as the incubation time increased. Since the real height of an adsorbed molecular arrangement on a surface can hardly be measured by AFM due to sample deformation (deformations up to 50% of the nominal value are reported for soft material[12,16]), the AFM height value could only be a fraction of the real height. Due to this reason, a direct correlation between the change in the AFM height value and the change in the molecular orientation cannot be drawn.

We applied RAIR spectroscopy, a widely used technique for acquiring information on the orientation of surface-immobilized molecules,[33,34] for developing an idea about the change in orientation of the sensor LNA probes with increasing incubation time. The RAIR spectra of the LNA layers on gold(111) surface for different incubation time periods 10 min, 30 min, 1 h, and 4 h are shown in Figure 5. In general, the peak intensities increased with increase in incubation time, which is not unexpected since the surface coverage increased as the incubation time was increased. However, consistent to the selection rule of RAIR spectroscopy, which states that "only vibrational modes with a dipole moment change normal to the surface will be active", clear changes in terms of the new bands appearing and some other bands disappearing, or bands becoming strikingly more intense, indicating LNA backbone reorientation with increase in incubation time, were observed. Five main absorption regions could be identified (a) the region 2997−2879 cm^{-1} for the C−H stretching frequencies,[35] (b) the

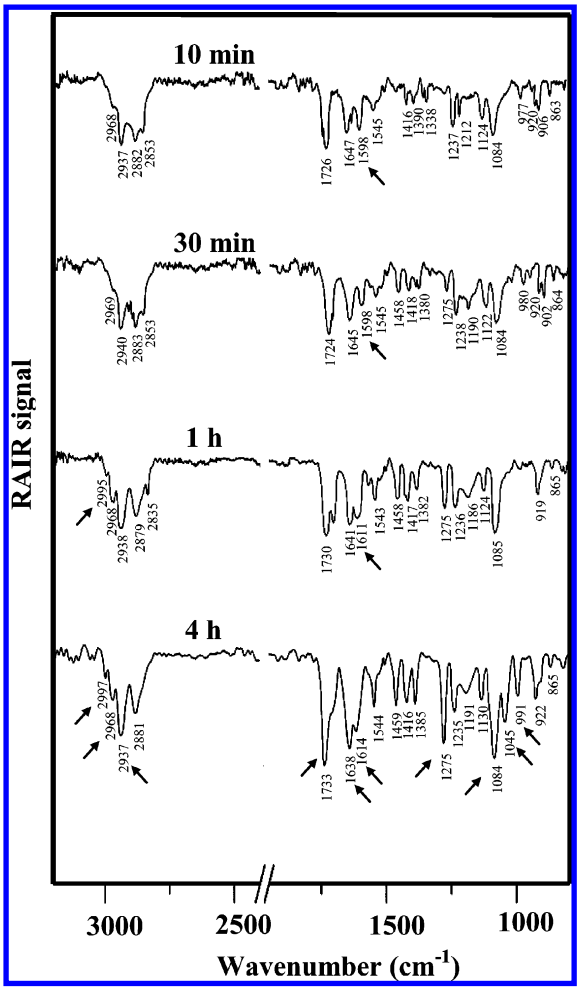

Figure 5. RAIR spectra obtained from the LNA SAM formed onto gold(111) surface. The concentration of LNA solution applied was 0.1 μM and four different incubation time periods were tested. The bands that undergo major changes indicating reorientation of LNA molecules are shown by arrows.

region 1733−1500 cm^{-1} for the nucleobase vibrations,[36] (c) the region 1500−1250 cm^{-1} for base-sugar vibrations, sensitive to glycosidic bond rotation, backbone conformation, and sugar puckering modes,[36] (d) the region 1250−1000 cm^{-1} for sugar−phosphate vibrations along sugar−phosphate chain, sensitive to nucleic acid backbone conformation,[36] (e) the region 1000−800 cm^{-1} for sugar vibrations, particularly sensitive to sugar puckering modes (N- and S-type).[36] The detail assignments of the bands are shown in Table 1. The absence of the S−H stretching frequency at ∼2550 cm^{-1} [37,38] indicates that there was no S−H linkage present in the system, meaning that LNA molecules were effectively immobilized onto gold substrate via gold−thiol bond formation. The relative changes in the band intensities/broadness were found to be generally correlative to the chemical structure of the LNA molecule. For example, the intensity of the 2940−2937 cm^{-1} band (for $-CH_2-$ groups) was found to be almost double than the intensity of the 2969−2968 cm^{-1} band (for $-CH_3$ groups) for all the incubation periods, which correlates to the presence of a greater number of $-CH_2-$ groups, compared to the $-CH_3$ groups. Also, the increase in the broadness of the $-CH_2-$ band could be correlated to the different $-CH_2-$ stretching modes from different sources (hexyl spacer/locked sugar) getting active as

dx.doi.org/10.1021/la204026j | Langmuir 2012, 28, 4325−4333

Table 1. Interpretation of the Primary IR Frequencies, Obtained from the RAIR Spectra of LNA SAM on Gold(111) Surface, with a Description of the Changes and the Incubation Times When the Changes Occur[a]

wavenumbers (cm^{-1})	interpretation with notable changes	time when this change is observed
2997−2995	$\nu(CH)_{aromatic}$, present in nucleobases,[35] appears and becomes stronger	from 1 h onward
2969−2968	$\nu_{asym}(CH_3)$, present in thymine bases,[35] becomes distinct and stronger	from 1 h onward
2940−2937	$\nu_{asym}(CH_2)$, present in hexyl spacer and locked sugar moieties,[35] broadened and becomes stronger	from 1 h, particularly at 4 h
2883−2879	$\nu_{sym}(CH_2)$,[35] broadened and becomes stronger	from 1 h onward
1733−1724	$\nu(C{=}O)$, present in thymine and guanine,[39,40] becomes stronger	from 1 h, particularly at 4 h
1647−1638	$\nu(C{=}O)$, present in cytosine and adenine,[39,40] becomes stronger	from 1 h, particularly at 4 h
1614−1611	$\delta(-NH_2)$, $\nu(C{=}N)$, present in nucleobases,[41] appears	from 1 h onward
1598	chemisorbed thymine,[42] disappears	from 1 h onward
1545−1543	$\nu(C{=}C)$, $\nu(C{=}N)$, present in nucleobases,[41] becomes stronger	from 1 h, particularly at 4 h
1459−1458	purine imidazolic ring vib.,[41] appears and becomes stronger	from 30 min, particularly at 4 h
1418−1416	sugar vib. (C3′- endo),[46−48] becomes stronger	from 1 h onward
1385−1380	glycosidic bond vib. of adenosines,[41] appears and becomes stronger	from 30 min, particularly at 4 h
1275	thymidine (N3−H bending vib.),[43] appears and becomes stronger	from 30 min, particularly at 4 h
1191−1186	sugar phosphate backbone vib. and N-type sugar conformation,[49] appears	from 30 min onward
1085−1084	$\nu_{sym}(PO_2^-)$,[44] becomes stronger	from 1 h onward
1045	$\nu(C{-}O)_{backbone}$,[45] appears	at 4 h
991−977	sugar−phosphate backbone vib.,[45] becomes stronger	particularly at 4 h
922−919	$\delta(N{-}H)_{oop}$, present in nucleobases,[41] becomes stronger	from 1 h onward

[a]The relevant references are shown in superscript against each interpretation.

the molecule reoriented more upright with increasing incubation time.

The spectral observations that most unambiguously indicated a major reorientation of the LNA molecules to the more upright one with increasing incubation times, especially 1 h onward, are highlighted in Figure 5. New bands in the regions 2997−2995 cm^{-1} and 1614−1611 cm^{-1} appeared and the bands in the region 2969−2968 cm^{-1} and 2940−2937 cm^{-1} became noticeably stronger from 1 h onward. The observations that a new peak appeared at 1045 cm^{-1} at the end of incubation of 4 h, and that the band in the region 991−977 cm^{-1} became strong only at this terminal stage of incubation, indicate that significant change of orientation toward the surface normal was achieved at the final stage of incubation. This is further supported by the observations that the bands/peaks in the regions 1733−1724 cm^{-1}, 1647−1638 cm^{-1}, 1275 cm^{-1} and 1085−1084 cm^{-1} all became significantly stronger at the end of 4 h incubation. Indications of a change toward more upright orientation at longer incubation times could be obtained also from the disappearance of the peak at 1598 cm^{-1} from 1 h onward.

Assessment of Hybridization Efficiency. To investigate the applicabilitiy of the LNA self-assembled monolayers as nucleic acid sensor films, the LNA-1 and LNA-2 modified gold substrates were subjected to treatment with the Cy3 labeled target DNA molecules (Cy3-DNA). After hybridization, the target DNA molecules were dehybridized by heating the gold pieces to 70 °C in sodium phosphate buffer solution. Then the gold pieces were taken out and the fluorescence intensity of the solutions containing the dehybridized Cy3-DNA probes was measured (for full experimental details, see Materials and Methods section). Complete removal of the labeled target DNA probes from the surface was checked by fluorescence imaging of each sample. It was observed that the fluorescence intensity of the target DNA solution, obtained from the fully matched duplex (LNA-1/Cy3-DNA), was significantly higher (50%) compared to that of the target DNA solution obtained from the duplex having single base mismatch (LNA-2/Cy3-DNA) (Figure 6a). Since in both cases, exactly same experimental protocol was applied, the difference in the fluorescence intensities observed could be attributed to the different amounts of the dehybridized target DNA strands obtained from the fully matched LNA-DNA duplexes and the duplexes having single base mismatch. This difference in the amount of the dehybridized target DNA probes indicate that the amount that was originally hybridized to the LNA sensor probes could be different for the fully matched and the singly mismatched situations. Previously, it has been shown by mass sensitive detection strategy that the amount of target molecules bound to the sensor molecules differed significantly between the fully complementary and singly mismatched situations.[50] In fact, a similar strategy as ours was earlier applied in a fluorescence-based study for assessment of the hybridization capacity of adsorbed oligonucleotides by Demers et al.[51]

When performance of the LNA SAM was compared to that of a DNA SAM by carrying out the exactly same kind of experiment and using the same base sequence as that of the LNA strands, the fluorescence intensity ratio complete match:single base mismatch was found to be about 1.5, in case of the LNA SAM, while it was 1.2 in case of the DNA SAM (Figure 6). This clearly indicated enhanced single base mismatch discrimination capability of the LNA layer compared to the DNA layer. The differences in the fluorescence intensities were determined on the basis of the intensity of the emission maximum and the percentage of fluorescence intensity increase for the complete match situation with respect to the single mismatch situation was estimated as about 50% in case of LNA whereas it was about 26% in case of DNA. The single base mismatch discrimination was therefore found to be enhanced about two times when LNA SAM was used. Since the absolute intensity values were also considerably higher (about 4−4.5 times) in case of the LNA SAM (Figure 6a) compared to those obtained from the DNA SAM measurements (Figure 6b), it is further indicated that the LNA SAMs could be more suitable for sensitive detection of nucleic acid targets, compared to the DNA SAMs.

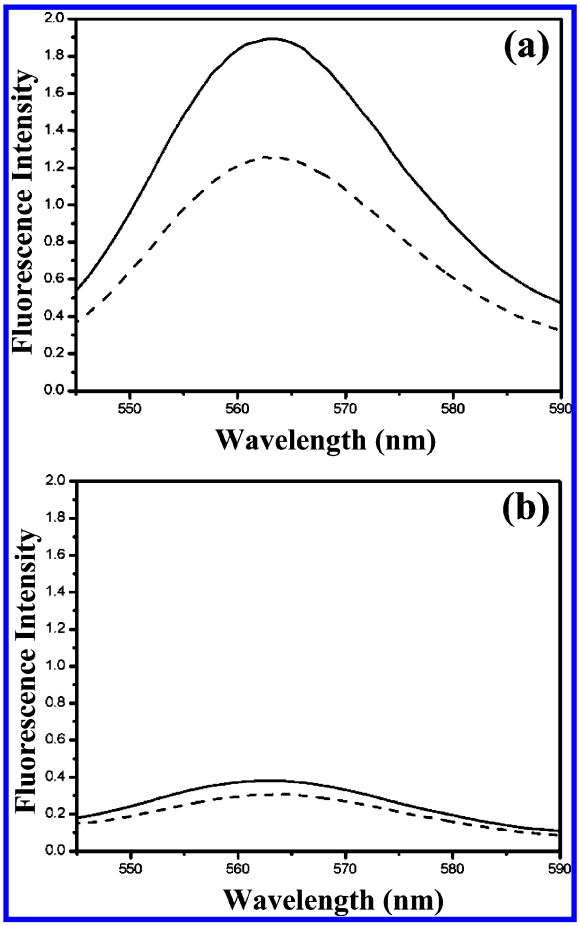

Figure 6. Fluorescence signals acquired from dehybridized target Cy3-DNA samples, where (a) LNA SAMs and (b) DNA SAMs are the relevant sensor layers. In both (a) and (b), the solid curves correspond to the signals acquired from the dehybridized Cy3-DNA, obtained from the fully complementary duplexes, while the dashed curves correspond to the signals acquired from the dehybridized Cy3-DNA, obtained from the singly mismatched duplexes.

DISCUSSION

In this study, we have shown that LNA molecules can self-assemble over a large area (7 μm × 7 μm) on gold(111) surface leading to formation of a two-dimensionally ordered bioactive monolayer. It is further shown that formation of such ordered LNA film depends on the choice of concentration of LNA molecules and incubation time. We did not observe an ordered arrangement in case of the DNA molecules (see Figure 1 in Supporting Information) under similar conditions as applied for LNA SAM formation. In fact, ordering of DNA molecules was not even expected, since electrostatic repulsion between the negatively charged ssDNA strands would prevent development of strand−strand proximity, which is an essential criterion for formation of a close-packed structure. However, in case of LNA, reproducible formation of a well-ordered arrangement of the molecules was observed, in spite of the fact that the LNA backbone is also negatively charged. The rigidity of the LNA backbone, introduced by the methylene bridge, which connects the 2′-oxygen and 4′-carbon of the sugar moieties, in effect resulting in a locked 3′-endo conformation and thereby reducing the conformational flexibility of the ribose units and increasing local organization of the phosphate backbone,[52] possibly somewhat compensated for the effects of electrostatic repulsion between the LNA strands. Nonspecific interaction between the adsorbate and the substrate, which is thought to be one of the primary reasons behind the difficulties in order formation, since random defects can be formed in the molecular layer due to nonspecific adsorption, could also be less in case of LNA compared to DNA, due to the structural rigidity of LNA backbone.[22] Other factors like presence of a large number of water bridges in the LNA strands,[23] compared to the DNA strands, could contribute in forming a barrier between the LNA nucleobases and the gold(111) surface, thereby lessening nonspecific adsorption (via gold−nitrogen interactions) of the LNA strands onto gold surface further. Two types of ordering of the LNA molecules were observed in the present study. First, one-dimensional molecule by molecule ribbonlike arrangement and second, two-dimensionally ordered assemblies formed due to parallel positioning of the ribbons. Though isolated molecules could be observed within the first 10 min of incubation (Figure 4a) and formation of the ordered SAMs took place within the first 30 min of incubation (Figure 4b and c), the upright orientation could be reached at an hours scale as evident from the RAIR spectra (Figure 5). This is in agreement to the fact that self-assembled monolayer formation occurs in two steps: an initial fast step of adsorption and a second slower step of monolayer organization.[53] Isolated features observed for the 10 min incubation stage might be due to the single LNA molecules. These features were of similar shapes and sizes having the AFM deconvoluted width value of 2.52 nm, which is in good agreement with the dimension of 2.6 nm of the energy minimized configuration of a LNA molecule (see Figure 2 and other relevant details in Supporting Information). The undeconvoluted size of the individual isolated LNA molecule was found to be about 14 nm, which was the same as the width of the ribbons, indicating that the ribbons were formed by molecule by molecule arrangement. One of the high-resolution images confirming this type of arrangement is shown in Figure 3b. It is likely that the basis of ribbon formation remained fixed throughout the study, since the width value of the LNA ribbons was found to be the same, that is, about 14 nm, always. The size of the individual molecular species also remained the same, i.e., 14 nm, throughout the study. The formation of the LNA ribbons and their parallel positioning could be a surface phenomenon, since had the ordered structures been formed in solution phase prior to LNA adsorption onto gold(111) surface, some ordered structures would have been observed at the initial stage of incubation, that is, for 10 min incubation. The LNA molecules were however observed in largely disordered manner at 10 min incubation stage (see Figure 4a) supporting the proposition of on-surface ordering. The ordered LNA SAM structures and a large degree of coverage of the SAM on gold(111) surface, as observed in the AFM images, might be related to application of a relatively flat and defect-free gold(111) substrate. In addition, the immersion incubation method that we applied for sample preparation, could offer additional advantage since the immersion method would not allow even partial drying of the sample and therefore would prevent nonspecific attachment of molecules on the surface to a significant extent. An obstruction to the thiol-specific adsorption of the other molecules, which is posed due to presence of the nonspecifically adsorbed molecules, could therefore be minimized. Events like intermolecular reorientation and arrangement, which are essential for ordering, are also possible only when the substrate surface is well-solvated and some extent of reversibility in

dx.doi.org/10.1021/la204026j | Langmuir 2012, 28, 4325−4333

chemisorption can be ensured. The advantage of immersion method, in comparison to other sample deposition methods where partial drying or complete drying may take place, has been exemplified in one earlier study.[32] Most importantly, the LNA film that was produced under the optimized preparation condition, reproducibly exhibited an enhanced single base mismatch discrimination capability in comparison to a DNA film formed under similar conditions (Figure 6). It has been observed earlier, in the solution phase experiments, that single base mismatch discrimination can be performed better using the LNA strands, compared to the DNA strands.[18,24] This superior discrimination capability of LNA has been attributed to the fact that LNA modifications enhance base stacking of fully matched base pairs and decrease stabilizing stacking interactions of mismatched base pairs.[54] This trend that is observed in the solution phase experiments has been reflected in case of the immobilized LNA strands onto gold(111) surface as shown in the present study. The trend could be reproduced on surface because the structural rigidity of the LNA backbone can result in reduced nonspecific interactions with the surface[22] helping the LNA strand to adopt more upright orientation and therefore making it least susceptible to the surface effects. The upright orientation also makes the LNA strand more accessible to the target DNA strand, ensuring greater fidelity in sequence recognition, therefore superior single base mismatch discrimination. On the other hand, the DNA sensor strands would be more susceptible to surface effects and at the same time, less accessible to the target strands since the DNA strands would lie close to the surface due to the nonspecific interactions. Lee et al. have in fact shown that the fluorescence of end-labeled DNA probes on gold substrate gets quenched by the surface, verifying that the strands lie close to the gold surface.[55] The fluorescence signal became stronger only when a mixed monolayer, using 11-mercapto-1-undecanol (MCU), was formed, prompting an upright orientation of the ssDNA strands, and moving the terminal fluorophore away from the substrate surface.

Recently, Wackerbarth et al. have shown that a duplex formed between thiol-DNA and LNA strands in solution, can significantly dissociate upon immobilization onto gold(111) surface, suggesting that significant unzipping of the duplexes can occur in order to achieve a high density of gold−sulfur bonds.[56] It seems that a better strategy to trap the duplexes onto the gold(111) surface could be to form a thiol-LNA SAM first and then expose the SAM to the target DNA molecules for hybridization to occur, as shown in the present study. More studies are however required to more precisely address the stability issues of the LNA-DNA duplexes on gold(111) surface. Our recent ongoing experiments (on the basis of melting point measurement of the surface-confined duplexes) indicate that formation of duplexes on the surface, rather than in solution, may be more advantageous, especially for single base mismatch discrimination, using thiol LNA compared to thiol DNA.

CONCLUSION

In conclusion, we report for the first time an investigation on a bioactive LNA SAM, which is prepared by simple immersion method and that consists of both one-dimensional and two-dimensional ordered arrangements of LNA molecules on gold(111) surface, by combined use of high-resolution AFM, RAIR spectroscopy, and fluorescence spectroscopy. The LNA molecules reached a suitably upright orientation at an hours scale. When compared to a DNA SAM prepared under similar conditions, the LNA SAM exhibited much superior detection ability in terms of target DNA detection and, especially, single base mismatch discrimination. Our findings suggest that LNA molecules can become a better candidate for simple and straightforward development of surface-based nucleic acid sensor assays, compared to DNA.

ASSOCIATED CONTENT

Supporting Information

AFM image of DNA-coated gold surface, molecular simulation of LNA molecule, and RAIR spectral assignment of the primary IR frequencies. This material is available free of charge via the Internet at http://pubs.acs.org.

AUTHOR INFORMATION

Corresponding Author

*Telephone: +91 33 2473 4971, Extn. 506. Fax: +91 33 2473 2805. E-mail: bcrm@iacs.res.in.

Notes

The authors declare no competing financial interest.

ACKNOWLEDGMENTS

We gratefully acknowledge the financial support (Grant No. BT/PR-11765/MED/32/107/2009) from Department of Biotechnology, Govt. of India; and the research fellowships of S.M. and S.G. from the Council of Scientific and Industrial Research, Govt. of India.

REFERENCES

(1) Li, Z. H.; Hayman, R. B.; Walt, D. R. Detection of Single-Molecule DNA Hybridization Using Enzymatic Amplification in an Array of Femtoliter-Sized Reaction Vessels. *J. Am. Chem. Soc.* **2008**, *130*, 12622.

(2) Kamahori, M.; Ishige, Y.; Shimoda, M. Detection of DNA hybridization and extension reactions by an extended-gate field-effect transistor: Characterizations of immobilized DNA-probes and role of applying a superimposed high-frequency voltage onto a reference electrode. *Biosens. Bioelectron.* **2008**, *23*, 1046.

(3) Briones, C.; Marti, E. M.; Navarro, C. G.; Parro, V.; Roman, E.; Gago, J. A. M. Ordered Self-Assembled Monolayers of Peptide Nucleic Acids with DNA Recognition Capability. *Phys. Rev. Lett.* **2004**, *93*, 208103.

(4) Berganza, J.; Olabarria, G.; Garcia, R.; Verdoy, D.; Rebollo, A.; Arana, S. DNA microdevice for electrochemical detection of Escherichia coli 0157:H7 molecular marker. *Biosens. Bioelectron.* **2007**, *22*, 2132.

(5) Kwon, Y-W; Lee, C. H.; Choi, D-H; Jin, J. I. Materials science of DNA. *J Mater. Chem.* **2009**, *19*, 1353.

(6) Arya, S. K.; Solanki, P. R.; Datta, M.; Malhotra, B. D. Recent advances in self-assembled monolayers based biomolecular electronic device. *Biosens. Bioelectron.* **2009**, *24*, 2810.

(7) Sharma, J.; Chhabra, R.; Andersen, C. S.; Gothelf, K. V.; Yan, H.; Liu, Y. Toward Reliable Gold Nanoparticle Patterning On Self-Assembled DNA Nanoscaffold. *J. Am. Chem. Soc.* **2008**, *130*, 7820.

(8) Love, J. C.; Estroff, L. A.; Kriebel, J. K.; Nuzzo, R. G.; Whitesides, G. M. Self-Assembled Monolayers of Thiolates on Metals as a Form of Nanotechnology. *Chem. Rev.* **2005**, *105*, 1103.

(9) Lang, H. P.; Hegner, M.; Meyer, E.; Gerber, Ch. Nanomechanics from atomic resolution to molecular recognition based on atomic force microscopy technology. *Nanotechnology* **2002**, *13*, R29−R36.

(10) Liu, M.; Amro, N. A.; Chow, C. S.; Liu, G. Production of Nanostructures of DNA on Surfaces. *Nano Lett.* **2002**, *2*, 863.

(11) Kasemo, B. Biological surface science. *Surf. Sci.* **2002**, *500*, 656.

(12) Herne, T. M.; Tarlov, M. J. Characterization of DNA Probes Immobilized on Gold Surfaces. *J. Am. Chem. Soc.* **1997**, *119*, 8916.

(13) Levicky, R.; Herne, T. M.; Tarlov, M. J.; Satija, S. K. Using Self-Assembly To Control the Structure of DNA Monolayers on Gold: A Neutron Reflectivity Study. *J. Am. Chem. Soc.* **1998**, *120*, 9787.
(14) Steel, A. B.; Herne, T. M.; Tarlov, M. J. Electrochemical Quantitation of DNA Immobilized on Gold. *Anal. Chem.* **1998**, *70*, 4670.
(15) Mourougou-Candoni, N.; Naud, C.; Thibaudau, F. Adsorption of Thiolated Oligonucleotides on Gold Surfaces: An Atomic Force Microscopy Study. *Langmuir* **2003**, *19*, 682.
(16) Wang, H.; Tang, Z.; Li, Z.; Wang, E. Self-assembled monolayer of ssDNA on Au(111) substrate. *Surf. Sci.* **2001**, *480*, L389.
(17) Casero, E.; Darder, M.; Díaz, D. J.; Pariente, F.; Martín-Gago, J. A.; Abruna, H.; Lorenzo, E. XPS and AFM Characterization of Oligonucleotides Immobilized on Gold Substrates. *Langmuir* **2003**, *19*, 6230.
(18) Singh, S. K.; Nielsen, P.; Koshkin, A. A.; Wengel, J. LNA (locked nucleic acids): synthesis and high-affinity nucleic acid recognition. *Chem. Commun.* **1998**, 455.
(19) Koshkin, A. A.; Nielsen, P.; Meldgaard, M.; Rajwanshi, V. K.; Singh, S. K.; Wengel, J. LNA (Locked Nucleic Acid): An RNA Mimic Forming Exceedingly Stable LNA:LNA Duplexes. *J. Am. Chem. Soc.* **1998**, *120*, 13252.
(20) Vester, B.; Wengel, J. LNA (Locked Nucleic Acid): High-Affinity Targeting of Complementary RNA and DNA. *Biochemistry* **2004**, *43*, 13233.
(21) Kurreck, J.; Wyszko, E.; Gillen, C.; Erdmann, V. A. Design of antisense oligonucleotides stabilized by locked nucleic acids. *Nucleic Acids Res.* **2002**, *30*, 1911.
(22) Martinez, K.; Estevez, M. -C.; Wu, Y.; Phillips, J. A.; Medley, C. D.; Tan, W. Locked Nucleic Acid Based Beacons for Surface Interaction Studies and Biosensor Development. *Anal. Chem.* **2009**, *81*, 3448.
(23) Pande, V.; Nilsson, L. Insights into structure, dynamics and hydration of locked nucleic acid (LNA) strand-based duplexes from molecular dynamics simulations. *Nucleic Acids Res.* **2008**, *36*, 1508.
(24) Ugozzoli, L. A.; Latorra, D.; Pucket, R.; Arar, K.; Hamby, K. Real-time genotyping with oligonucleotide probes containing locked nucleic acids. *Anal. Biochem.* **2004**, *324*, 143.
(25) Fritz, J.; Baller, M. K.; Lang, H. P.; Rothuizen, H.; Vettiger, P.; Meyer, E.; Güntherodt, H.-J.; Gerber, Ch.; Gimzewski, J. K. Translating Biomolecular Recognition into Nanomechanics. *Science* **2000**, *288*, 316.
(26) Mukhopadhyay, R.; Lorentzen, M.; Kjems, J.; Besenbacher, F. Nanomechanical Sensing of DNA Sequences Using Piezoresistive Cantilevers. *Langmuir* **2005**, *21*, 8400.
(27) Drummond, T. G.; Hill, M. G.; Barton, J. K. Electrochemical DNA sensors. *Nat. Biotechnol.* **2003**, *21*, 1192.
(28) Hansen, J. A.; Mukhopadhyay, R.; Hansen, J. O.; Gothelf, K. V. Femtomolar Electrochemical Detection of DNA Targets Using Metal Sulfide Nanoparticles. *J. Am. Chem. Soc.* **2006**, *128*, 3860.
(29) Sanborn, M. E.; Connolly, B. K.; Gurunathan, K.; Levitus, M. Fluorescence Properties and Photophysics of the Sulfoindocyanine Cy3 Linked Covalently to DNA. *J. Phys. Chem. B* **2007**, *111*, 11064.
(30) Jia, K.; Wan, Y.; Xia, A.; Li, S.; Gong, F.; Yang, G. Characterization of Photoinduced Isomerization and Intersystem Crossing of the Cyanine Dye Cy3. *J. Phys. Chem. A* **2007**, *111*, 1593.
(31) Nuzzo, R. G.; Allara, D. L. Adsorption of Bifunctional Organic Disulfides on Gold Surfaces. *J. Am. Chem. Soc.* **1983**, *105*, 4481.
(32) Ghosh, S.; Mukhopadhyay, R. An atomic force microscopy investigation on self-assembled peptide nucleic acid structures on gold(111) surface. *J. Colloid Interface Sci.* **2011**, *360*, 52.
(33) Young, J. T.; Boerio, F. J.; Zhang, Z.; Beck, T. L. Molecular Structure of Monolayers from Thiol-Terminated Polyimide Model Compounds on Gold. 1. A Spectroscopic Investigation. *Langmuir* **1996**, *12*, 1219.
(34) Trenary, M. Reflection Absorption Infrared Spectroscopy and the Structure of Molecular Adsorbates on Metal Surfaces. *Annu. Rev. Phys. Chem.* **2000**, *51*, 381.
(35) Silverstein, R.; Webster, F. *Spectroscopic Identification of Organic Compounds*, 6th ed.; John Wiley & Sons Inc: New York, 2006; Chapter 3.
(36) Banyay, M.; Sarkar, M.; Gräslund, A. A library of IR bands of nucleic acids in solution. *Biophys. Chem.* **2003**, *104*, 477.
(37) Ihs, A.; Liedberg, B. Chemisorption of L-Cysteine and 3-Mercaptopropionic Acid on Gold and Copper Surfaces: An Infrared Reflection-Absorption Study. *J. Colloid Interface Sci.* **1991**, *144*, 282.
(38) Manna, A.; Imae, T.; Yogo, T.; Aoi, K.; Okazaki, M. Synthesis of Gold Nanoparticles in a Winsor II Type Microemulsion and Their Characterization. *J. Colloid Interface Sci.* **2002**, *256*, 297.
(39) Wang, Z.; Liu, D.; Dong, S. In-situ FTIR study on adsorption and oxidation of native and thermally denatured calf thymus DNA at glassy carbon electrodes. *Biophys. Chem.* **2001**, *89*, 87.
(40) Yamada, T.; Shirasaka, K.; Takano, A.; Kawai, M. Adsorption of cytosine, thymine, guanine and adenine on Cu(1 1 0) studied by infrared reflection absorption spectroscopy. *Surf. Sci.* **2004**, *561*, 233.
(41) Mateo-Martí, E.; Briones, C.; Pradier, C. M.; Martín-Gago, J. A. A DNA biosensor based on peptide nucleic acids on gold surfaces. *Biosens. Bioelectron.* **2007**, *22*, 1926.
(42) Petrovykh, D. Y.; Kimura-Suda, H.; Whitman, L. J.; Tarlov, M. J. Quantitative Analysis and Characterization of DNA Immobilized on Gold. *J. Am. Chem. Soc.* **2003**, *125*, 5219.
(43) Liquier, J.; Akhebat, A.; Taillandier, E.; Ceolin, F.; Huynh Dinh, T.; Igolen, J. Characterization by FTIR spectroscopy of the oligoribonucleotide duplexes r(A-U)$_6$ and r(A-U)$_8$. *Spectrochim. Acta* **1991**, *47A*, 177.
(44) Shimanouchi, T.; Tsuboi, M.; Kyogoku, Y. In *The Structure and Properties of Biomolecules and Biological Systems, Advances in Chemical Physics*; Duchesne, J., Eds.; Interscience: London, 1964; p 435.
(45) Tsuboi, M. In *Applied Spectroscopy Reviews*; Brame, E. G. J., Eds.; Dekker: New York, 1969; p 45.
(46) Taillandier, E.; Liquier, J. Infrared spectroscopy of DNA. *Methods Enzymol.* **1992**, *211*, 307.
(47) Liquier, J.; Taillandier, E. In *Infrared Spectroscopy of Biomolecules*; Mantsch, H. H., Chapman, D., Eds.; Wiley-Liss, Inc: New York, 1996; p 131.
(48) Taillandier, E.; Peticolas, W. L.; Adam, S.; Huynh-Dinh, T.; Igolen, J. Polymorphism of the d(CCCGCGGG)$_2$ double helix studied by FT-i.r. spectroscopy. *Spectrochim. Acta* **1990**, *46A*, 107.
(49) Pohle, W.; Fritzsche, H. A new conformation-specific infrared band of A-DNA in films. *Nucleic Acids Res.* **1980**, *8*, 2527.
(50) Okahata, Y.; Kawase, M.; Niikura, K.; Ohtake, F.; Furusawa, H.; Ebara, Y. Kinetic Measurements of DNA Hybridization on an Oligonucleotide-Immobilized 27-MHz Quartz Crystal Microbalance. *Anal. Chem.* **1998**, *70*, 1288.
(51) Demers, L. M.; Mirkin, C. A.; Mucic, R. C.; Reynolds, R. A.; Letsinger, R. L.; Elghanian, R.; Viswanadham, G. A Fluorescence-Based Method for Determining the Surface Coverage and Hybridization Efficiency of Thiol-Capped Oligonucleotides Bound to Gold Thin Films and Nanoparticles. *Anal. Chem.* **2000**, *72*, 5535.
(52) Braasch, D. A.; Corey, D. R. Locked nucleic acid (LNA): fine-tuning the recognition of DNA and RNA. *Chem. Biol.* **2001**, *8*, 1.
(53) Schwartz, D. K. Mechanisms and Kinetics of Self-Assembled Monolayer Formation. *Annu. Rev. Phys. Chem.* **2001**, *52*, 107.
(54) You, Y.; Moreira, B. G.; Behlke, M. A.; Owczarzy, R. Design of LNA probes that improve mismatch Discrimination. *Nucleic Acids Res.* **2006**, *34*, e60.
(55) Lee, C. Y.; Gong, P.; Harbers, G. M.; Grainger, D. W.; Castner, D. G.; Gamble, L. J. Surface Coverage and Structure of Mixed DNA/Alkylthiol Monolayers on Gold: Characterization by XPS, NEXAFS, and Fluorescence Intensity Measurements. *Anal. Chem.* **2006**, *78*, 3316.
(56) Wackerbarth, H.; Grubb, M.; Wengel, J.; Chorkendorff, Ib.; Ulstrup, J. Adsorption and surface dynamics of short DNA and LNA oligonucleotides on single-crystal Au(111) electrode surfaces. *Surf. Sci.* **2006**, *600*, L122.